Original article

The three-dimensional structure of vascular smooth muscle cells: a confocal laser microscopic study of rabbit mesenteric arterioles

Atsushi Nakano[a], Motomu Minamiyama[b], Junji Seki[c]

[a]*Departments of Vascular Physiology* [c]*Department of Bioengineering, National Cardiovascular Center Research Institute, Osaka 565-8565,* [b]*Department of Clinical Engineering, Hiroshima International University, Higashi-Hiroshima 724-0695, Japan*

Background: Information of the three dimensional (3D) structure of vascular smooth muscle cells (VSMCs) is essential for understanding the regulatory mechanism of blood flow in the microvascular system.
objective: To examine the 3D structure of individual VSMCs in rabbit mesenteric arterioles, using confocal laser scanning microscopy.
Methods: Japanese white rabbits were anesthetized with urethane and α-chlorase. After intravital observation of the mesenteric microcirculation under a videomicroscope, the intestine with mesentery was extracted and perfused and fixed with paraformaldehyde under a static pressure (100 mmHg). A section of the mesentery was isolated from the intestine and spread out to simulate the *in vivo* geometry of the the vascular network. The mesenteric section was stained with fluorescein anti-smooth muscle myosin antibody and rhodamine-labeled anti-rabbit Ig antibody. The samples were observed using confocal laser microscopy, and the 3D images were reconstructed by means of sliced images. The cross-sectional image was re-sliced to measure two axes of the best-fitting ellipse. Single VSMCs were picked out from the vascular wall using the continuity law of density distribution of vessel wall.
Results: The cross-sectional shapes of arterioles were not circular but elliptical. The aspect ratio (major to minor axis) of the best-fitting ellipse was in the range from 0.3 to 0.7 for 28 arterioles (diameters: 10-30 µm). On the 3D image of VSMCs, the cell width ranged from 2.2 to 4.5 µm. The cells were classified into round and spindle types. The cell width of round shape was significantly larger than that of spindle shape. The VSMCs appeared to arrange circumferentially and tightly along the cross-section along the axis of vessel. The mean length of single VSMCs was approximately 1.2 times of the circumferential length of the arteriole. This cellular arrangement may have influence on the distribution of mechanical stress by VSMC-induced myogenic force.
Conclusion: Confocal laser microscopy is useful for quantitative analysis of the 3D arrangement of individual VSHCs.

Keywords: Arteriole, cellular arrangement, confocal laser microscopy, cross-sectional shape, mesentery, vascular smooth muscle cell.

A number of factors are involved in regulation of blood flow in organs and tissues [1, 2], an important one being vascular smooth muscle cells (VSMCs). Single VSMCs in microvessels are very long and narrow with longitudinal grooves (or striations), arranged along the circumference of the vascular wall [3, 4]. VSMCs can induce vasodilation/vasoconstriction by changing their tone [5,6]. Mechanical stresses induced on the wall by VSMCs are influenced by the cellular arrangement as well as the microvascular cross-sectional shape. Therefore, accurate information on the three-dimensional (3D) structure of single

Correspondence to: Dr. Atsushi Nakano, Department of Vascular Physiology, National Cardiovascular Center Research Institute, Suita, Osaka 565-8565, Japan; E-mail: nakano@ri.neve.go.jp

VSMCs is essential for understanding the regulatory mechanism of blood flow in the microvascular system.

The microvasculature can be visualized and observed *in vivo* under a fluorescence microscope. However, the microscopic images cannot provide accurate information of the cross-section or the 3D structure or arrangement of VSMCs. There are several studies using corrosion casts or angiography of microvasculature, on the microvascular network and microvascular architecture in various organs and tissues [7-10]. However, they cannot provide information of the 3D arrangement of individual VSMCs and the cross-sectional shape of micro-vessels.

Recently, confocal laser microscopy has been developed to obtain the 3D images of microvascular wall and various cells in the microvasculature [11-16]. In a previous paper, we studied the 3D structure of rat mesenteric arterioles using confocal laser microscopy [15]. The purpose of this paper is to investigate the 3D morphological structure of arteriolar walls in rabbit mesentery, using confocal laser microscopy. We performed quantitative analysis of the 3D arrangement of individual VSMCs associated with the cross-sectional shape.

Materials and methods
Animal preparation

Japanese white rabbits (male, 1.6-1.9 kg body weight) were used in accordance with the Guiding Principles for the Care and Use of Animals in the Field of Physiological Sciences (published by the Physiological Society of Japan). The rabbits (n=15) were anesthetized with urethane (70 mg/kg body weight) and α-chloralose (30 mg/kg body weight) intraperitoneally, and allowed to respire spontaneously. A carotid artery was cannulated to monitor blood pressure during the experiment. The intestinal mesentery was exteriorized from an abdominal incision, and placed into a bath, which was perfused with Krebs-Ringer solution (KRS) (37 °C, pH 7.35), and spread out on an observation window on a microscopic stage.

Morphological examination

Harvest of the microvasculature. The rabbits were sacrificed after the *in vivo* observation. The rabbit intestine with mesentery was extracted, and was kept at 4 °C during the harvest of the microvasculature. Under a static perfusion pressure of approximately 100 mmHg, the intestinal vasculature was perfused from the superior mesenteric artery with KRS to flush out the blood, and then perfused with 2 % paraformaldehyde (PFA) for 5 min to fix the tissue. The effluent was drained from the catheter in the superior mesenteric vein. The microvasculature was harvested. Two or three triangular sections of the mesentery were isolated from the intestine. After the sample was treated with Dispase (1 mg/mL) at 37°C for 30 minutes, a mixture of 0.2 % Polyoxyethylene Octylpheny Ether (NP-40) and 2 % PFA was superfused to remove the cell membrane and to fix the sample for 30 minutes. The micro-vasculature was stained just after the harvest, and analyzed within two days as described below.

Immunochemical staining. The section of mesentery was spread out to simulate the 2D *in vivo* geometry of the vascular network. The spread section was pinned on a paraffin sheet in shale filled with KRS, so that the geometry of microvascular network is preserved. Actin fibers (such as stress fiber) of the section were stained with fluorescein phalloidin for subsequent excitation with blue light (B-excitation, wavelenght=488 nm). Smooth muscle myosin was stained by indirect fluorescence immunological method using anti-smooth muscle myosin antibody (rabbit, affinity purified) and rhodamine-labeled with anti-rabbit Ig antibody (goat) for the green (G) excitation (wavelength=546 nm).

Confocal microscopy. The stained mesentery section was observed under a confocal laser scanning microscope (CLSM). The CLSM consisted of a fixed stage microscope (Olympus BX50WIFI), a scanning system (Olympus Fluoview FV300) and laser units (488 nm blue argon-ion and 546 nm green helium-neon). An objective lens (x60, N.A.0.9, water-immersion; Olympus LUMPlan FL60W) was used. For the vertical scanning, a piezo positioner was mounted to the objective lens. A scanning image size was set at 512x512 pixels with the resolution of 0.3x0.3 m^2 pixel, where the observation area had a size of approximately 150x150 μm^2. By using a piezo positioner, 50-80 slices of images were selected with 0.6 μm interval (the thickness of observed volume: 30-50 μm) to reconstruct the 3D volume of microvessel. Based on the obtained confocal slice images, the 3D volume of microvessel was reconstructed with 0.3x0.3x0.6 μm^3 voxel, using AVS (Ver.5.0, Advanced Visual Systems,USA). The cross-sectional images of arterioles were re-sliced from the reconstructed volume with 5 mm interval to characterize the structure and topology of arteriolar wall.

Image analysis

Sampling. Twenty-six arterioles were selected out of 15 rabbit mesenteries, where diameters ranged from 10 to 25 μm.

Procedure of image analysis. For confocal microscopic observations of stained arterioles, B-excitation or G-excitation images were used to examine the arrangements of actin fibers or smooth muscle myosin, respectively. A set of the sliced data of cross-sectional image were separated into images of 12bit TIFF (tagged image file format) images, which were post-analyzed using Photoshop (Adobe, Ver.6.02, USA). Using the AVS, we reconstructed a 3D volume of arteriole, which can be rotated to any direction and sliced at right-angled cross-sections with accuracy of less than 5 degrees.

Images of the cross-section. In each vessel, 4-5 cross-sections were taken perpendicular to the axis of vessel, and based on the 3D reconstructed image, and representative cross-sectional images were used for the analysis. The luminal surface of vessel cross-section was traced with the freehand selection tool using the NIH Image software (Ver.1.6.3, National Institute of Health, USA). By applying a best-fitting ellipse to the traced lumen, we determined the two principal axes (2*a* and 2*b*) of the ellipse using the NIH image measurement command (see **Fig. 1**). The best-fitting ellipse was defined by equating the second order central moments of the ellipse to the trace. These semi-manual image processing procedures were done by two persons, and the measurement results were averaged. Then, the aspect ratio (α), mean diameter (Dm) and circumferential length (L) were calculated as follows:
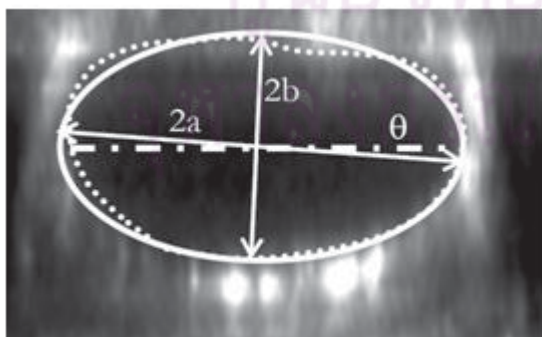

Fig. 1 Tracing of the vessel lumen and best-fitting of ellipse to the traced lumen, based on the image. The 2*a* and 2*b* are two principal axes of the best-fitting ellipse.

$$\alpha = b / a , \tag{1}$$
$$Dm = 2(ab)^{1/2}, \tag{2}$$
$$L = \pi(a+b)\{1+(1/4)\,\kappa^2+(1/64)\,\kappa^4+....\}, \tag{3}$$
$$\text{and} \quad \kappa = (a-b)/(a+b). \tag{3.a}$$

The α term indicates the degree of elliptic flatness, and $0<\alpha<1.0$; α =1.0 corresponds circular shape of the cross-section and $\alpha<1.0$ means collapse of the cross-section. Equation (3) is rewritten in terms of α as follows:

$$L= \pi Dm\,(1/2)\,(\alpha^{1/2}+1/\alpha^{1/2})(\{1+(1/4)\,\kappa^2+(1/64)\,\kappa^4+..\}, \tag{4}$$
$$\kappa=(1-\alpha)/(1+\alpha). \tag{4.a}$$

Images of microvascular wall with VSMCs. Based on the confocal slice images (G-excitation image), the 3D volume of microvascular wall was reconstructed. The 3D morphological structures of single VSMC, such as shape, arrangement and width, were evaluated on the reconstructed images.

Images of individual VSMC were classified into two types: round and spindle shapes as shown in **Fig. 2** (**A**, **B**). Selecting sections of images where more than 10 VSMCs were arranged in parallel to each others, we calculated their mean cellular width (*MCW*) as follows:

$$MCW= \text{(Measured length) / (Total number of cells)}. \tag{5}$$

Images of individual VSMCs in vascular walls. To examine the morphological features of single VSMCs, we picked out single cells from the vascular wall by means of the density distribution of images. For this purpose, we evaluated the density distribution of images in the vascular wall by using the AVS, and then we identified the 3D region, based on the continuity of density between the upper and lower area. Finally, we obtained 3D cellular images of single cells.

Results

3D reconstructed images

Figure 3 shows a sequence of 47 sliced confocal images of a single arteriole with smooth muscle myosin stained, and its reconstructed image. VSMCs were characterized by a spiral structure along the circumference of vessel. The spiral structure was not uniform along the axis of vessel; its pitch may be either tight or loose along the axis of vessel.
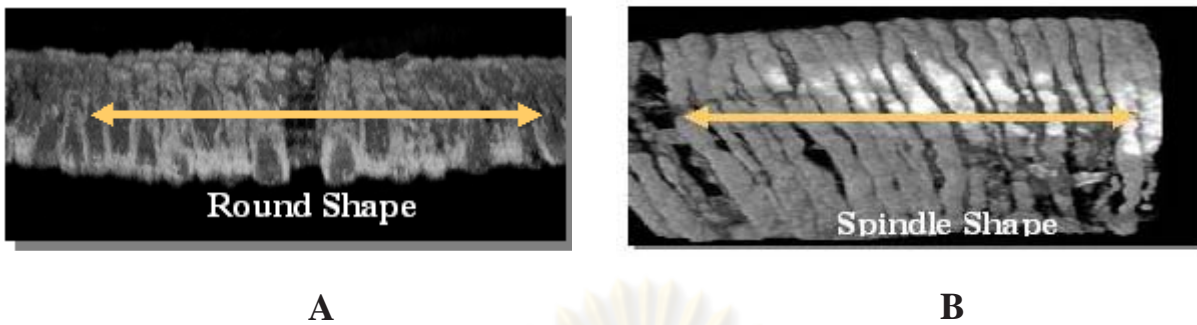
Fig. 2 Two types of VSMC morphology observed from the 3D confocal images of rabbit mesenteric arterioles (**A**: round shape and **B**: spindle shape).
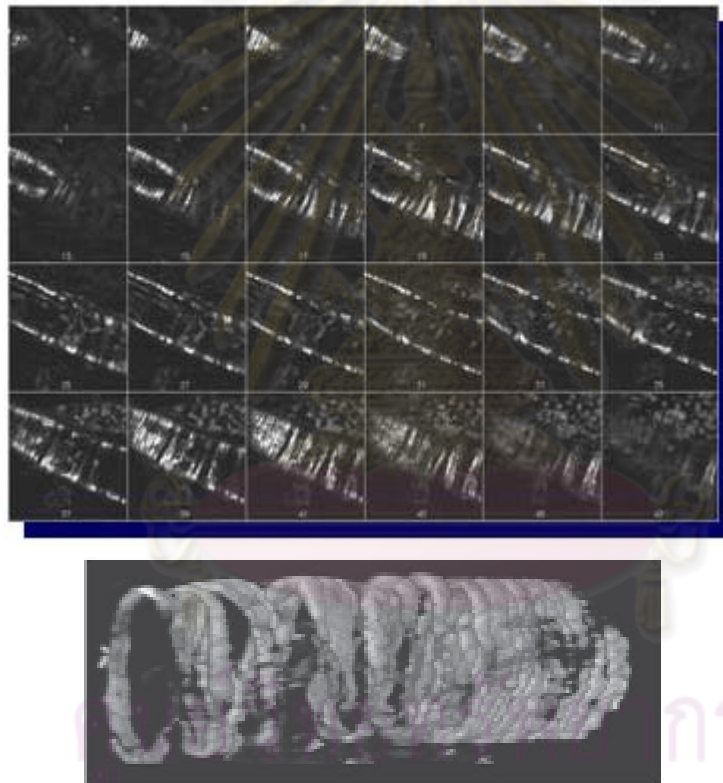

Fig. 3 A sequence of sliced confocal images (indirect fluorescence immunochemical staining) (upper figures; 1-47: slice images obtained at each 1.8 μm thickness) and the 3D reconstructed image (lower figure) of an arteriole with VSMC myosin stained in the rabbit mesentery.

There appeared to be a variety of morphological shapes of VSMCs, based on the 3D reconstructed images of microvascular walls. In single arterioles, two types of VSMCs were observed; one was round shaped and the other spindle shaped, as seen in **Fig. 2**. The round types resemble tear-drops with clear nuclei, while spindle-shaped types were more string-like.

The 3D images of VSMCs showed a complicated morphology at bifurcations or side-branches (**Fig. 4**). It is apparent from the figures that VSMCs are arranged tightly, showing some discontinuity at the bifurcation or side-branches. The VSMCs were of spindle shape in the upper figure, and of round shape in the lower figure.
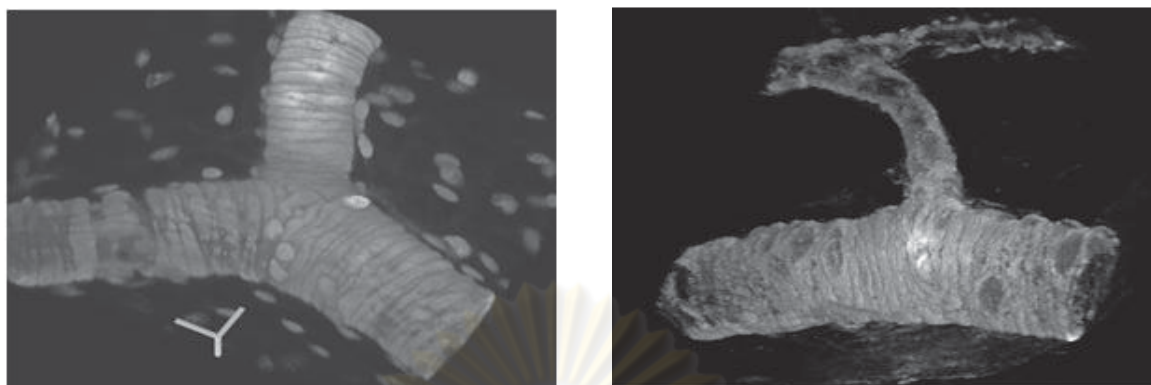
Fig. 4 Cellular arrangements of VSMCs in the arteriolar wall around bifurcation (left figure) and side- branching (right figure).

Cross-sections of mesenteric arterioles

Twenty six arterioles were measured in 15 mesenteries. The major and minor diameters of the best fitting ellipse were plotted in **Fig. 5**. The aspect ratio (α) ranged from 0.3 to 0.7, indicating that mesenteric arterioles were flattened horizontally. The mean aspect ratio averaged over 26 arterioles was:

$$\text{Mean aspect ratio} = 0.47 \quad 0.10 \, (\text{mean} \quad \text{SD}, n=26). \quad (6)$$

The aspect ratio (α) and the circumferential length (L) were plotted against the mean diameter (Dm) in **Figs. 6** and **7**. The aspect ratio fell in the range from 0.3 to 0.7 in single arterioles. The circumference lengths were linearly proportional to the mean diameters.

Cellular width of VSMCs in arterioles

As has been previously mentioned, the 3D reconstructed image of VSMCs demonstrated two basic shapes: round and spindle-like (**Fig. 2**). The

mean VSMC width (*MCW*) was measured from the 3D reconstructed images of single arterioles and branched arterioles; for the single arterioles, the VSMCs were further classified into either round or spindle-shaped. The measured *MCWs* were plotted against the mean diameter (Dm) in **Fig. 8**.

The MCW ranged from 2 to 4.5 mm in single arterioles, while it fell in the range from 3 to 4.5 μm in branched arterioles. The relationship between MCW and the circumferential length (L) is seen in **Fig. 6**. It did not appear that the MCW was correlated with the mean diameter (Dm) or the circumferential length (L).

Figure 9 shows histogram of two shapes (round and spindle) of VSMCs against the *MCW*.

The peak appeared near MCW=2.5 μm for spindle shaped VSMCs, while it was at 4.5 μm for round shaped VSMCs. Interestingly, the mean cell width of round shaped VSMCs was significantly larger than that of the spindle shaped.
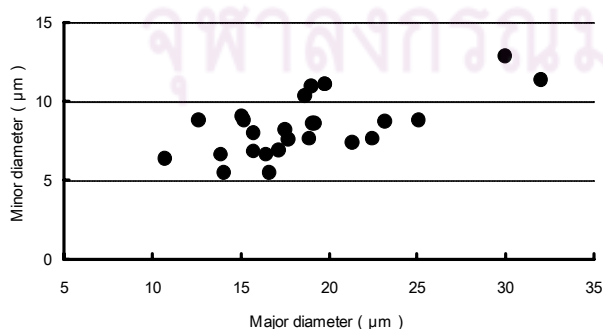

Fig. 5 Major (2*a*) and minor diameter (2*b*) of the best-fitting ellipses measured in 26 single arterioles.
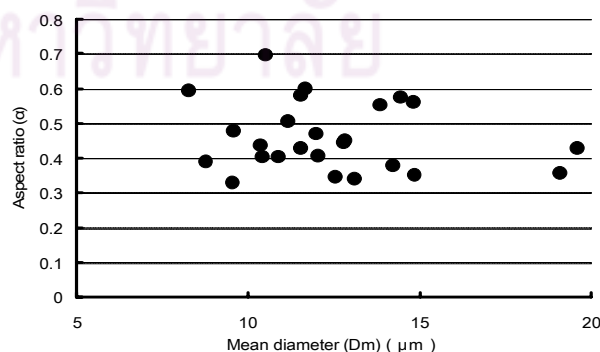

Fig. 6 Aspect ratio (α) of the cross-section of arterioles against the mean diameter (Dm) measured in 26 single arterioles.
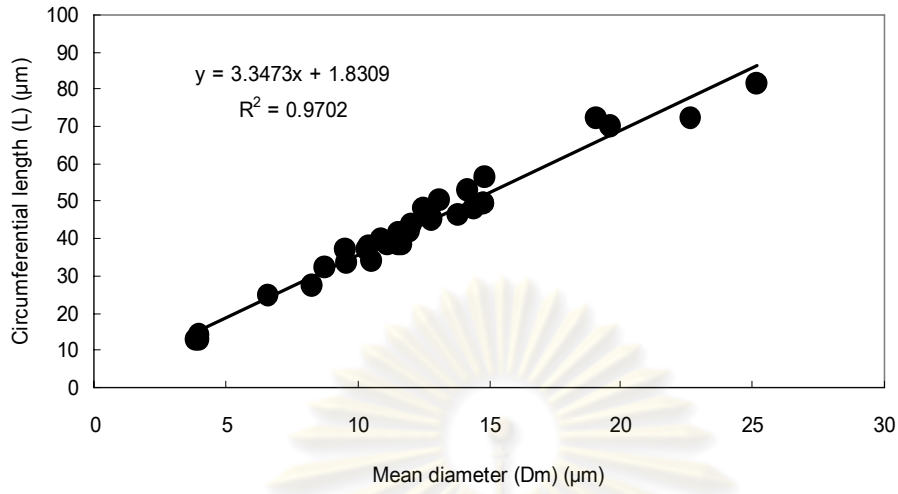
Fig. 7 Circumferential lengths (L) against the mean diameter (Dm) in 26 single arterioles. The solid line indicates the linear regression line.
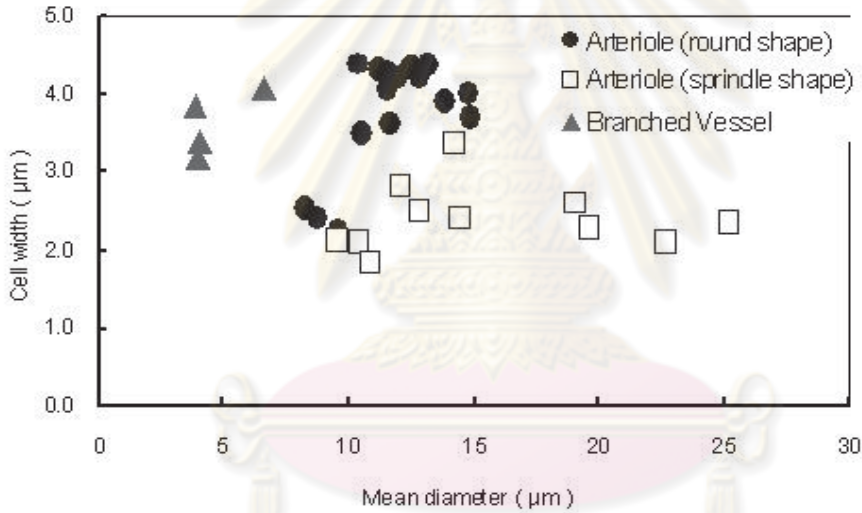

Fig. 8 Mean cell widths (MCW) of single VSMCs (round and spindle shape) against mean diameters (Dm) in 26 single arterioles and 4 side-branched arterioles. The MCW (y) is related to Dm (x) by the following regression lines: $y=0.23x+1.04$ ($R^2=0.39$) for round shape (indicated by solid line), and $y = 0.0024x + 2.38$ ($R^2=0.0009$) for spindle shape (indicated by dotted line).
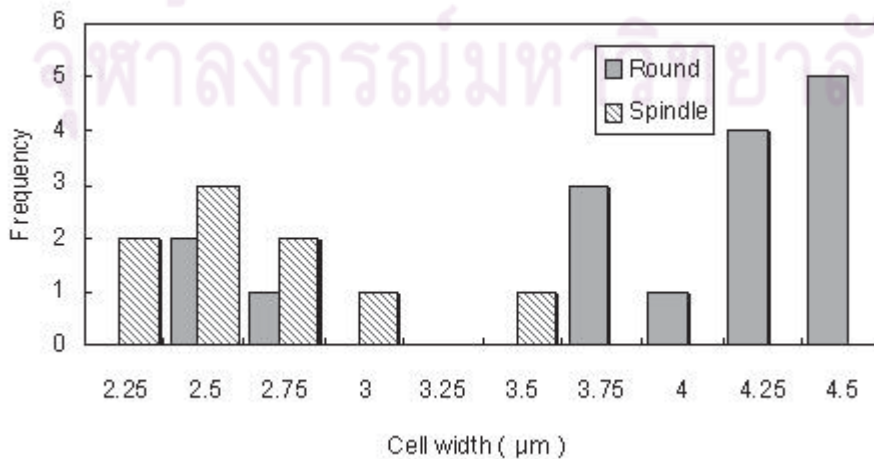

Fig. 9 Histogram of VSMCs (round and spindle shape) against the cell width (MCW) in single arterioles (round shape n=17, and spindle shape n=9).

The *MCW* of single and branched arterioles were calculated in 15 rabbit mesenteries and tabulated in **Table 1.**

The 3D structure of arteriolar wall

By using the NIH image program, we obtained cross-sectional images of the arteriolar wall at different planes of rotation. Figure 10 shows nine images of cross-sections viewed on different planes of 20° rotation (each). Among these cross-sectional images, 80° and 100° rotational images show highly flattened (or elliptic-like) shapes of cross-section. Other images (0°-60° and 120°-160° rotational) demonstrate how VSMCs are distributed discontinuously and nonuniformly along the axis of vessel. Interestingly, some discontinuity appeared in VSMC distribution in the vascular wall. The morphology of individual VSMCs was surveyed in the longitudinal direction by rotating the 3D image of arteriolar wall. Most VSMCs appeared to cover the vascular wall about 1.5 times along the circumference.

For qualitatively evaluating the longitudinal features of individual VSMCs along the circumference of vascular wall, single VSMCs were picked out from the vascular wall images used in **Fig.10**. **Fig. 11** shows images of four single VSMCs (**a**-**d**) superimposed on the image used in **Fig. 10** (upper figure) and the cross-sectional image of the cell **d** (lower figure). These selected single VSMCs were of elliptic-like cross-sectional shape, and their terminals were very thin and of anchor-like shape. For these single cells (**a**-**d**), the circumferential length was measured to compare with the circumferential length of arteriole. The mean circumferential length of single VSMCs was approximately 1.2 times of the circumferential length of arteriole.

Discussion

Intravital microscopic observations examine *in vivo* structures of endothelial cells [17] or VSMCs [18] as well as the morphology of microvascular networks [19]. However, intravital microscopy provides only the 2D images of microvessels [19-22]. Scanning electron scanning microscopy (SEM) can also be used to observe the structure of vascular cells (endothelial cell or VSMCs) [3, 23-27], but it cannot provide the 3D image of single cells. The present confocal laser microscopy enables us to provide the 3D images of the microvascular wall.

Table 1. Mean SMC width (MCW) in single and branched arterioles measured in 15 rabbit mesenteries. (Data are expressed in mean SD).

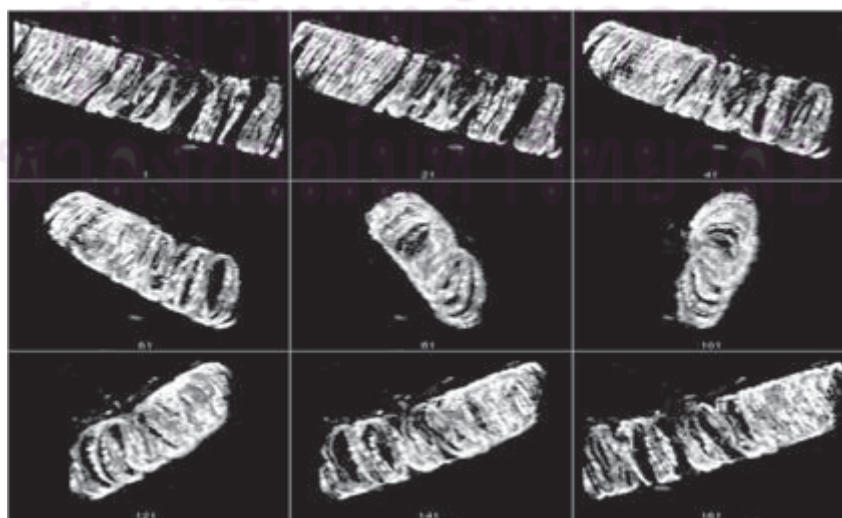|	Single arteriole		Branched arteriole
	Round shape VSMC	Spindle shape VSMC	
Mean cell width (μm)	3.78 0.73 (n=16)	2.59 0.71 (n=12)	3.63 0.40 (n=4)

Fig. 10 Cross-sectional images (1-9) viewed at different angles (reconstructed using the NIH image program).

The cross-section of mesenteric arteries was of elliptic shape. Its aspect ratio (major to minor axis) was 0.48 in the average, indicating that the arterioles were of horizontally flattened shape. The elliptic-like shape might be due to anisotropic distribution of external pressure against the external surface [16].

A variety of morphologies appear in cultured VSMCs [28-30]. The present study classified the cells into two types (round and spindle shapes). For the round shape, the cellular width increased with an increase in the diameter of arterioles. For the spindle shape, on the other hand, the width remained almost constant. Most cells of the round shape were from the smaller diameter of arterioles, compared to the spindle-shaped. The cellular width of the round shape was significantly larger than that of the spindle shape (**Fig. 9**, **Table 1**).

We could pick out single VSMCs from the 3D images of vascular wall. The selected cell images demonstrated that individual VSMCs were arranged almost perpendicular to the axis of vessel (**Fig. 11**). Several previous studies indicate different angles of cell orientation to the axis of vessel in various vessels. Azuma *et al* examined the morphology of VSMCs in dog artery and vein histologically [31, 32]. The VSMCs were arranged helically (or spirally) along the axis of vessel. The more peripheral was the portion of the vessel chosen, the more turns in the VSMC spiral and the less the value of the angle. Todd *et al.* made SEM examination of alignment of VSMCs in rat vessels. The VSMCs were aligned at a steeper angle in the vessel wall (15±2º) of the muscular artery than in those with more elastic tissue (9±2º) [33]. According to Takamizawa & Hayashi, VSMCs in rabbit carotid arteries were orientated almost perpendicular to the axis of vessel [34].

We have examined the length and width of single VSMCs by rotating the obtained 3D image of individual cells (**Figs.10** and **11**). The VSMCs were 1.2 times long, compared to the circumference of the arteriole, indicating them to be about 75 μm longer and 4 μm wide. These values are in agreement with ones estimated by Uehara *et al* [4].

In views of biomechanics of VSMCs, it is important to examine: i) whether one VSMC covers the entire circumference of the arterioles, and ii) whether two neighboring VSMCs are attached to each other or not. In the present confocal microscopic observation, two neighboring VSMCs were arranged almost in parallel with each other; moreover their terminals were not close together. Furthermore, there was a VSMC-poor area in the vascular wall (indicated by the discontinuity of the cell distribution along the axis of vessel in **Fig. 10**). These findings indicate that no connection existed in the terminals of two adjacent cells.

The 3D morphological structure of VSMCs has influence on hemodynamic variables such as blood pressure and flowing shear stress. Van Gieson *et al* reported an increase in VSMC coverage of microvessels exposed to increased stress *in vivo* [35]. The present confocal microscopic images have demonstrated peculiar arrangements of VSMCs at bifurcations and side-branchings (**Fig. 4**), which may be closely related with the flow patterns at these special regions [36-38].

In the present study, we report a new technique developed so that single VSMCs from the vascular wall may be individually studied. In the near future, the technique will be improved to obtain more clear images for quantitative analysis of VSMC structural changes in the microvasculature.
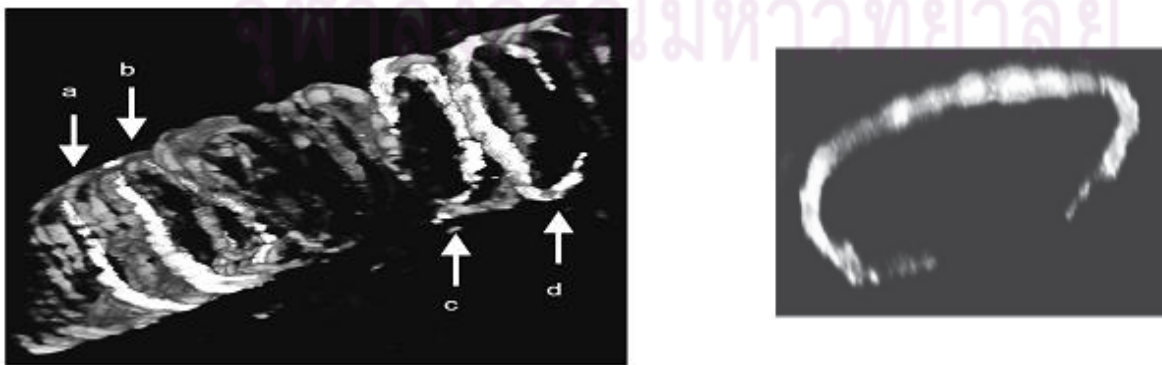

Fig. 11 Detection of single VSMCs from the arteriolar wall used in **Fig. 10**. The left figure: images of four single VSMCs (**a-d**) superimposed on the image of **Fig. 10**; the right figure: cross-sectional image of the cell **d**.

References

1. Baskurt OK, Yalcin O, Meiselman HJ. Hemorheology and vascular control mechanisms. Clin Hemorheol Microcirc. 2001;30:169-78.

2. Niimi H. Microcirculatory control in the brain tissue. In: Kamada, Shiga, McCuskey, eds.Tissue Perfusion and Organ Function: Ischemia/Reperfusion Injury. Amsterdam:Elsevier Science; 1996.p.49-59.

3. Uehara Y, Suyama K. Visualization of the adventitial aspect of the vascular smooth muscle cells under the scanning electron microscopy. J Electron Microsc (Tokyo). 1978;27:157-9.

4. Uehara Y. Morphology of vascular smooth muscle fibers and pericytes. In: Motta PM, editor. Ultrastructure of smooth muscle. Boston:Kluwex; 1990. p. 237.

5. Brekke JF, Gokina NI, Osol G. Vascular smooth muscle cell stress as a determinant of cerebral artery myogenic tone. Am J Physiol Circ Physiol. 2002;283: H2210-H2216.

6. Sleek GE, DulingBR. Coordination of mural elements and myofilaments during arteriolar constriction, Circ Res. 1986;59:620-7.

7. Bhutto IA, Amemiya T. Microvascular architecture of the rat choroid: corrosion cast study. Anat Rec. 2001; 264:63-71.

8. Hashimoto H, Ishikawa H, Kusakabe M. Three-dimensional investigation of vascular nets by fluorochrome-labeled angiography. Microvasc Res. 1998;55:179-83.

9. Ikebe T, Shimada T, Ina K, Kitamura H, Nakatsuka K. The three-dimensional architecture of retinal blood vessels in KK mice, with special reference to the smooth muscle cells and pericytes. J Electron Microsc (Tokyo). 2001;50:125-132.

10. Lametschwandtner A, Minnich B, Kachlik D, Setina M, Stingl J. Three-dimensional arrangement of the vasa vasorum in explanted segments of the aged human great saphenous vein: scanning electron microscopy and three-dimensional morphometry of vascular corrosion casts. Anat Rec. 2004;281: 1372-82.

11. He P, Adamson RH. Visualization of endothelial cleft and nuclei in living microvessels with combined reflectance and fluorescence confocal microscopy. Microcircul. 1995;2:267-76.

12. Jariyapongskul A, Nakano A, Yamaguchi S, Nageswari K, Niimi H. Maturity of pericytes in cerebral neocapillaries induced by growth factors. Clin Hemorheol Microcirc. 2003;29:417-21.

13. Saino T, Satoh Y. Application of real-time confocal laser scanning microscopy to observe living cells in tissue specimens. J Electron Microsc (Tokyo). 2004; 53:49-56.

14. Hamid SA, Howe DC, Cambell S, Daly CJ. Visualisation of morphological changes in living intact human microvessels using confocal microscopy. Microvasc Res. 2005;69:173-77.

15. Nakano A, Minamiyama M, Niimi H. Cross-sectional shape of rat mesenteric arterioles at branching studies by confocal laser scanning microscopy. JSME Intern J. 2006;49 (Ser C): 240-6.

16. Dickie R, Bachoo RM, Rupnick MA, Dallabrida SM, DeLoid GM, Lai J, et al. Three dimensional visualization of microvessel architecture of whole-mount tissue by confocal microscopy. Microvasc Res. 2006;72:20-6.

17. Adamson RH. Microvascular endothelial cell shape and size in situ. Microvasc Res. 1993;46:77-88.

18. Minamiyama M, Nakano A, Hanai S, Masuda M. In vivo observation of vascular smooth muscle cells at the arteriol-precapillary bifurcation in the mesentery under fluorescence video microscopy. Microcircul annual. 1995;11:193-4.

19. Tozer GM, Ameer-Beg SM, Baker J, Barber PR, Hill SA, Hodgkiss RJ, et al. Intravital imaging of tumour vascular networks using multi-photon fluorescence microscopy. Adv Drug Deliv Rev. 2005;57:135-52.

20. Kiani MF, Cokelet GR, Sarelius IH. Effect of diameter variability along a microvessel segment on pressure drop. Microvasc Res. 1993;45:219-32.

21. Pries AR, Schonfeld D, Gaehtgens P, Kiani MF, Cokelet GR. Diameter variability and microvascular flow resistance. Am J Physiol Circ Physiol. 1997;272: H2716-H2725.

22. Yamaguchi S, Yamakawa T, Niimi H. Cell-free plasma layer in cerebral microvessels, Biorheol. 1992;29: 251-60.

23. Coats P, Jarajapu YP, Hillier C, McGrath JC, Daly C. The use of fluorescent nuclear dyes and laser scanning confocal microscopy to study the cellular aspect of arterial remodeling in human subjects with critical limb ischemia. Exp Physiol. 2003;88:547-54.

24. Evan AP, Connors BA. Morphometric analysis of vascular smooth muscle cells by scanning electron microscopy. Int Rev Exp Pathol. 1996;36:31-52.

25. Krizmanich WJ, Lee RM. Correlation of vascular smooth muscle cell morphology observed by scanning electron microscopy with transmission electron microscopy. Exp Mol Pathol. 1997;64:157-72.

26. Krizmanich WJ, Lee RM. Scanning electron microscopy of vascular smooth muscle cells from

spontaneously hypertensive rats. Scanning Microsc. 1993;7:129-34.

27. Miller BG, Gattone VH, Overhage JM, Bohlen HG, Evan AP. Morphological evaluation of vascular smooth muscle cell: length and width from a single scanning electron micrograph of microvessels. Anat Rec. 1986;216:95-103.

28. Grunwald J, Schaper W, Mey J, Hauss WH. Special characteristics of cultured smooth muscle cell subtypes of hypertensive and diabetic rats. Artery 1982;11:1-14.

29. Lau HK. Regulation of proteolytic enzymes and inhibitors in two smooth muscle cell phenotypes. Cardiovasc Res. 1999;43:1049-59.

30. Sas DF, Lundy JK, Miller LJ. Culture of human neoplastic gastrointestinal smooth muscle cells. In Vitro Cell Dev Biol. 1989;25:730-36.

31. Azuma T, Hasegawa M. A rheological approach to the architecture of arterial walls. Jpn J Physiol. 1971; 21:27-47.

32. Azuma T, Hasegawa M. Distensibility of the vein: from the architectural point of view, Biorheol. 1973; 10:469-79.

33. Todd ME, Laye CG, Osborne DN. Dimensional characteristics of smooth muscle in rat blood vessels: a computer-assisted analysis. Circ Res. 1983; 53: 319-31.

34. Takamizawa K, Hayashi K, Matsuda T. Isometric biaxial tension of smooth muscle in isolated cylindrical segments of rabbit arteries. Am J Physiol Circ Physiol. 1992;263:H30-H34.

35. Van Gieson EJ, Murfee WL, Skalak TC, Price RJ. Enhanced smooth muscle cell coverage of micro-vessels exposed to increased hemodynamic stresses in vivo. Circ Res. 2003;92:929-36.

36. Kalsho G, Kassab GS. Bifurcation asymmetry of the porcine coronary vasculature and its implications on coronary heterogeneity. Am J Physiol Circ Physiol. 2004;287:H2493-H2500.

37. Minamiyama M, Hanai S. Propagation property of vasomotion at terminal arterioles and precapillaries in the rabbit mesentery. Biorheol. 1991;28:275-86.

38. Nakano A, Sugii Y, Minamiayma M, Niimi H. Measurement of red cell velocity in microvessels using particle image velocimetry (PIV). Clin Hemorheol Microcirc. 2003;29:445-55.